Electrophysiological Identification of α- and β-Intercalated Cells and Their Distribution along the Rabbit Distal Nephron Segments

S. Muto, K. Yasoshima,* K. Yoshitomi,* M. Imai,* and Y. Asano
*Departments of Nephrology and *Pharmacology, Jichi Medical School, Minamikawachi, Kawachi, Tochigi, 329-04 Japan*

Abstract

By cable analysis and intracellular microelectrode impalement in the in vitro perfused renal tubule, we identified α- and β-intercalated (IC) cells along the rabbit distal nephron segments, including the connecting tubule (CNT), the cortical collecting duct (CCD), and the outer medullary collecting duct in the inner stripe ($OMCD_i$). IC cells were distinguished from collecting duct (CD) cells by a relatively low basolateral membrane potential (V_B), a higher fractional apical membrane resistance, and apparent high Cl^- conductances of the basolateral membrane. Two functionally different subtypes of IC cells in the CCD were identified based on different responses of V_B upon reduction of the perfusate Cl^- from 120 to 12 mM: the basolateral membrane of β-IC cells was hyperpolarized, whereas that of α-IC cells was unchanged. This is in accord with the hypothesis that the apical membrane of β-IC cells contains some Cl^--dependent entry processes, possibly a Cl^-/HCO_3^- exchanger. Further characterization of electrical properties of both subtypes of IC cells were performed upon lowering bath or perfusate Cl^- from 120 to 12 mM, and raising bath or perfusate K^+ from 5 to 50 mM. A 10-fold increase in the perfusate K^+ had no effect on V_B in both subtypes of IC cells. Upon abrupt changes in Cl^- or K^+ concentration in the bath, a large or a small depolarization of the basolateral membrane, respectively, was observed in both subtypes of IC cells. The electrical properties of α- and β-IC cells were similar among the distal nephron segments, but their distribution was different: in the CNT, which consists of IC cells and CNT cells, 97.3% (36/37) of IC cells were of the β type. In the CCD, which consists of IC cells and CD cells, 79.8% (79/99) of IC cells were of the β-type, whereas in the $OMCD_i$ 100% (19/19) were of the α type, suggesting that the β type predominates in the earlier and the α type in the later segment. (*J. Clin. Invest.* 1990. 86:1829–1839.) Key words: bicarbonate secretion • chloride, isolated perfused tubule • microelectrode • proton secretion

Introduction

The distal nephron segments of the mammalian kidney, including the distal convoluted tubule (DCT),[1] connecting tubule (CNT), and collecting ducts (CD), play major roles in the ultimate regulation of Na^+, K^+, water, and the acid–base balance.

Although the DCT consists of a single type of cells, the other segments consist of heterogenous cells. In the CNT, CNT cells and intercalated (IC) cells are intermingled, whereas the cortical and outer medullary portions of the collecting duct are the mixture of CD cells and IC cells (1). In order to understand precisely the functions of these segments, it is necessary to clarify the transport properties of individual type of cell.

The CNT cells (2–4) as well as CD cells (5–18) primarily appear to be mainly responsible for the transport of Na^+ and K^+, whereas less numerous IC cells (6, 8, 10, 11, 14, 18, 19) are thought to be responsible for H^+, HCO_3^-, and Cl^- transport. The microelectrode studies have characterized the electrical membrane properties of these three distinct cell types (4, 8, 18). The cells of the inner stripe of the outer medullary collecting duct ($OMCD_i$) is specialized by H^+ secretion (20–24) and their electrical properties have also been defined (25).

Stetson and Steinmetz (26) reported that in the turtle urinary bladder, there are at least two subtypes of IC cells, α- and β-IC cells. Morphologic and immunocytochemical studies have indicated that the similar subtypes also exist in the mammalian collecting ducts (10, 14, 27–35). The α-IC cells secrete H^+ and reabsorb HCO_3^-. The HCO_3^- exit is via a basolateral Cl^-/HCO_3^- exchanger, which is immunologically similar to the Cl^-/HCO_3^- exchanger of the mammalian red blood cell, band 3 protein (28, 30), and is sensitive to the disulfonic stilbens (28). In contrast, the β-IC cells reabsorb H^+ via an H^+ pump in the basolateral membrane, and secrete HCO_3^- via a Cl^-/HCO_3^- exchanger in the apical membrane, which binds peanut lectin (28, 30) and is resistant to the disulfonic stilbens (28). More recently, several investigators (34–36), using fluorescent cell pH measurement, identified two subtypes of the IC cells in the rabbit cortical collecting duct (CCD). However, no information is available for the electrophysiological differentiation of two subtypes of IC cells. Recently, Yoshitomi et al. (4) reported that IC cells can be identified by electrophysiological means also in the CNT, but their exact subtype was unknown. The present study was designed to identify α- and β-IC cells electrophysiologically and to characterize their electrical properties along the distal nephron segments.

Our results indicate that two functionally different subpopulations of IC cells were identified and their distribution along the distal nephron segments was heterogeneous.

Address reprint requests to Dr. Muto, Department of Nephrology, Jichi Medical School, Minamikawachi, Kawachi, Tochigi, 329-04 Japan.

Received for publication 26 April 1990 and in revised form 2 August 1990.

1. *Abbreviations used in this paper:* CCD, cortical collecting duct; CD cell, collecting duct cell; CNT, connecting tubule; DCT, distal convoluted tubule; fR_A, fractional apical membrane resistance; IC cell, intercalated cell; $OMCD_i$, outer medullary collecting duct in the inner stripe; R_T, transepithelial resistance; V_B, basolateral membrane voltage; V_T, transepithelial voltage.

J. Clin. Invest.

0021-9738/90/12/1829/11 $2.00
Volume 86, December 1990, 1829–1839

Methods

Isolation and perfusion of tubules. Female Japanese white rabbits weighing 1.5–2.0 kg were maintained on standard rabbit chow and tap water ad lib. After the animals were anesthetized with pentobarbital (35 mg/kg, i.v.), both kidneys were removed. Slices of the coronary section 1–2 mm thick were made and transferred to a dish containing a cold intracellular fluid–like solution of the following composition: 14 mM KCl, 44 mM K_2HPO_4, 14 mM KH_2PO_4, 9 mM $NaHCO_3$, and 160 mM sucrose.

Three different distal nephron segments, including the CNT, CCD, and $OMCD_i$, were isolated by identifying them according to the criteria previously reported (1, 2, 25). Then, the isolated nephron segment was perfused in vitro according to the method of Burg et al. (37) with slight modifications. Briefly, the tubule segment was perfused via a perfusion pipette inserted into one end of the tubule. A PE-10 tube (Intramedic, Clay Adams, Parsippany, NJ) was inserted into the perfusion pipette to permit rapid exchange of the perfusate with a test solution within 5 s. The opposite or distal end of the tubule was held in a glass holding pipette with a small amount of Sylgard 184 (Dow Corning Corp., Midland, MI). The perfusion flow rates were > 15 nl/min and controlled by the height of the outflow sink.

The tubule was perfused in the bathing chamber of ~ 100 μl to permit rapid exchange of the bathing solution within 5 s. The bathing solution flowed at 5–15 ml/min from the reservoirs by gravity through a water jacket to permit the bath temperature to be regulated at 37°C.

Electrical measurements. The transepithelial and cellular electrical properties of the tubule were measured using techniques described previously (5, 8, 12, 18, 25, 38) with slight modifications. Briefly, the perfusion pipette was connected through an agar bridge (3% agar in 3 M KCl) to a calomel half-cell electrode. Bathing fluid was also connected through an agar bridge (3% agar in 3 M KCl) to another grounded calomel half-cell electrode. The transepithelial voltage (V_T) was measured with a dual-channel electrometer (KS-700, WP Instruments, Inc., New Haven, CT), and recorded on a four-pen chart recorder (R64, Rikadenki, Tokyo, Japan).

The transepithelial resistance (R_T) was measured by cable analysis undertaken by injecting constant-current pulses, ΔI_0, 50–100 nA (300 ms in duration, 10-s intervals) into the tubule lumen via the perfusion pipette. The resulting voltage deflections at the perfusion end, ΔV_0, were recorded via the salt bridge and electrometer noted above. At the distal end of the tubule, the voltage deflections, ΔV_L, resulting from the injection of the constant-current pulses were measured via a calomel half-cell electrode connected to the tubular fluid accumulating in the holding pipette through an agar bridge. The luminal length constant (λ) determined by

$$L/\lambda = \cosh^{-1}(\Delta V_0/\Delta V_L), \quad (1)$$

where L is the length of the tubule. R_T is obtained from

$$R_T = 2\pi r\lambda(\Delta V_0/\Delta I_0)\tanh(L/\lambda), \quad (2)$$

where r is the apical radius of the tubule.

Conventional microelectrodes were fabricated from borosilicate glass capillaries (1.2 mm OD, 0.6 mm ID; Frederick Haer & Co., Brunswick, ME) by using a vertical puller (PE-2, Narishige, Tokyo, Japan). Microelectrodes were filled with 0.5 M KCl and connected to one channel of a high-input impedance electrometer (Duo 773, WP Instruments, Inc.) via a holder having Ag-AgCl pellets. Microelectrode resistance was between 80 and 150 MΩ. The basolateral membrane voltage (V_B) was measured by impaling a cell with an electrode.

Fractional resistance of the apical membrane (fR_A) was estimated as

$$fR_A = R_A/(R_A + R_B) = 1 - \Delta V_B/\Delta V_X, \quad (3)$$

where R_A and R_B are the resistance of the apical and basolateral membranes, respectively, and ΔV_B and ΔV_X are the voltage deflections during luminal current injection across the basolateral cell membrane and at the site of microelectrode puncture from the perfusion end, respectively. The deflections of transepithelial voltage (ΔV_X) at the point of cellular impalement was estimated as

$$\Delta V_X = \Delta V_0 \cosh(X/\lambda - L/\lambda)/\cosh(L/\lambda), \quad (4)$$

where X is the distance between the perfusion pipette and the point of impalement with the microelectrode.

Identification of the IC cell and characterization of the electrical properties of different cell types. IC cells were electrophysiologically distinguished from other cell types by a relatively low V_B and high fR_A, as described in several previous papers by Muto et al. (8) and Koeppen (18, 25). They were also differentiated by different V_B responses upon step changes in bath K^+ and Cl^- concentration. Thus, to identify the different cell types and better characterize their electrical properties of apical and basolateral membranes, the bathing or perfusing solutions were rapidly changed by lowering Cl^- from 120 to 12 mM (cyclamate substitution) or raising K^+ from 5 to 50 mM (Na replacement), as shown in Table I.

Solutions. The composition of all solutions is listed in Table I. Each had an osmolality between 285 and 295 msmol/kg of H_2O and was equilibrated at 37°C with 95% O_2/5% CO_2.

Statistical analysis. All values are expressed as means±SE. Comparison between two groups was made by a paired t test.

Results

Electrical profiles and cable properties of CNT, CCD, and $OMCD_i$ segments

Table II summarizes electrical profiles and cable properties determined when each nephron segment was perfused with a symmetrical control solution (Table I). The V_T and R_T obtained from the CNT and CCD are consistent with those previously reported (4, 5, 8, 12). The R_T obtained from the $OMCD_i$ in the present study, 293.5 Ω·cm², was lower than that reported by Koeppen (25) in this segment, 534 Ω·cm². The reason for this difference is unknown.

Identification of the IC cell in the CCD

At first, we electrophysiologically identified the CD cell and the IC cell in the CCD, according to the criteria described previously (see Methods). As shown in Fig. 1, we observed two distinct populations based on the values of V_B and fR_A: one

Table I. Composition of Solutions

	Control	50 mM K^+	12 mM Cl^-
		mM	
Na^+	146.8	91.8	146.8
K^+	5.0	50.0	50.0
Ma^{2+}	1.0	1.0	1.0
Ca^{2+}	1.8	1.8	1.8
Cl^-	120.6	120.6	12.0
HCO_3^-	25.0	25.0	25.0
Acetate	10.0	10.0	10.0
HPO_4^{2-}	0.8	0.8	0.8
$H_2PO_4^-$	0.2	0.2	0.2
Cyclamate			108.6
L-Alanine	5.0	5.0	5.0
D-Glucose	8.3	8.3	8.3

All solutions were gassed with 95% O_2–5% CO_2 at 37°C.

Table II. Electrical Profiles and Cable Properties of CNT, CCD, and $OMCD_i$ Segments

Parameters	CNT	CCD	$OMCD_i$
Tubules (n)	64	98	12
Transepithelial voltage, V_T (mV)	−9.9±0.9	−7.4±0.7	7.5±1.6
Cable analyses (n)	8	75	10
Tubular length, L (μm)	425.6±65.1	801.3±30.2	641.0±60.1
Length constant, λ (μm)	154.3±26.4	297.2±12.3	279.8±15.1
Tubular radius, r (μm)	13.7±0.5	14.1±0.2	15.5±0.5
Transepithelial resistance, R_T ($\Omega \cdot cm^2$)	39.7±6.7	111.7±6.8	293.5±37.6

Values are mean±SE.

group[2] had a higher V_B (−81.8±1.4 mV, n = 38) and a lower fR_A (0.33±0.04, n = 38), and the other group had a lower V_B (−28.3±1.1 mV, n = 86) and a higher fR_A (0.95±0.003, n = 86). The former cell type was compatible with the CD cell, whereas the latter was identified as the IC cell. These findings are in good agreement with those reported in several previous papers reported by Muto et al. (8) and Koeppen (18, 25).

Evidence for two subtypes of IC cells in the CCD

During random impalements of IC cells, we noticed that upon reduction of the perfusate Cl^- from 120 to 12 mM, some IC cells exhibited a hyperpolarization of the basolateral membrane, whereas others did not. These two distinct responses were sometimes observed in the same tubule. Fig. 2 illustrates representative recordings in which two different responses were observed in the same CCD segment. The latter cell type was identified as the α-IC cell because of the absence of a Cl^- entry step at the apical membrane. The former cell type was identified as the β-IC cell because of the presence of a process that is dependent on luminal Cl^- concentration. This distinction of β- from α-IC cells by the presence or the apparent absence of apical Cl^- entry process is based on previously deduced IC cell models (10, 14, 26–36, 40). Since both subtypes of IC cells were observed in the same tubule, the observation reflects true cellular heterogeneity within the same segment rather than variations among the tubules or animals.

We examined the effect of reduction of the perfusate Cl^- concentration on V_B of IC cells in the CCD as identified by the criteria mentioned above. The frequence distribution of the deflection of V_B is shown in Fig. 3. It is clear from this figure that there are two groups of cells having different responses to the reduction of the luminal Cl^- concentration. There was no overlap of the values between two groups. Therefore, the cell which hyperpolarized by > 8 mV was defined as the β-IC cell.

Properties of the apical and basolateral membranes of the α- and β-IC cells in the CCD

The electrical properties of the apical and basolateral membranes of these two subtypes of IC cells were further characterized by observing changes in V_B upon changing ion concentrations in the perfusate or in the bath.

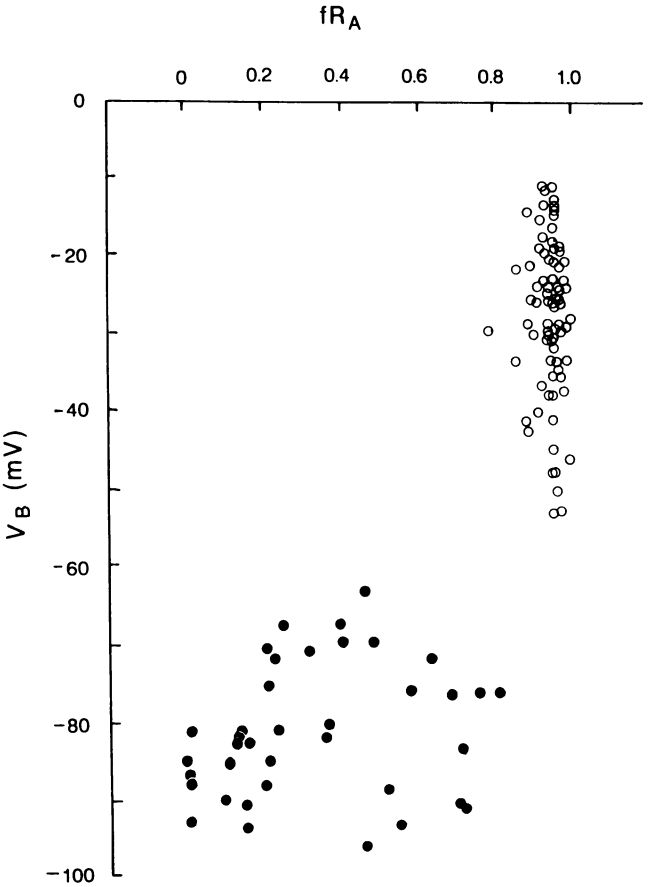

Figure 1. Discrimination of CD cells and IC cells with two electrophysiologic parameters, V_B and fR_A. (●) CD cells; (○) IC cells.

α-IC cell. The α-IC cells had a mean V_B of −27.1±2.1 mV (n = 29). The fR_A was near unity and averaged 0.94±0.01 (n = 26). In view of the extremely high values of fR_A, it seems that the apical membrane of the α-IC cell contains no appreciable ion conductances. To rule out the presence of significant conductive pathway for K^+ in this membrane we observed V_B by raising K^+ concentration in the perfusate from 5 to 50 mM.

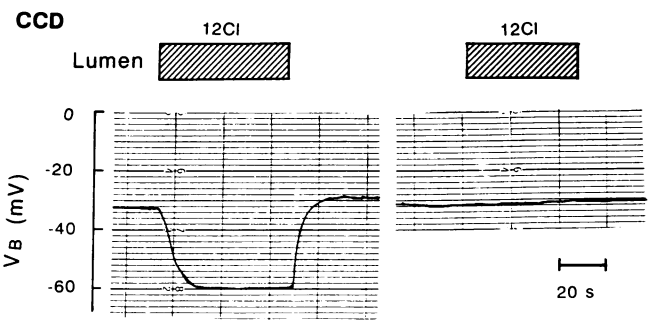

Figure 2. Representative tracings of V_B showing two different V_B responses in the same CCD segment upon reduction of the perfusate Cl^- from 120 to 12 mM.

2. Because we focused on the IC cells of the CCD, we did not necessarily take data when we impaled CD cells. Therefore, the frequency of the CD cell in the present study does not correspond to that reported previously in the rabbit CCD (1, 11, 39).

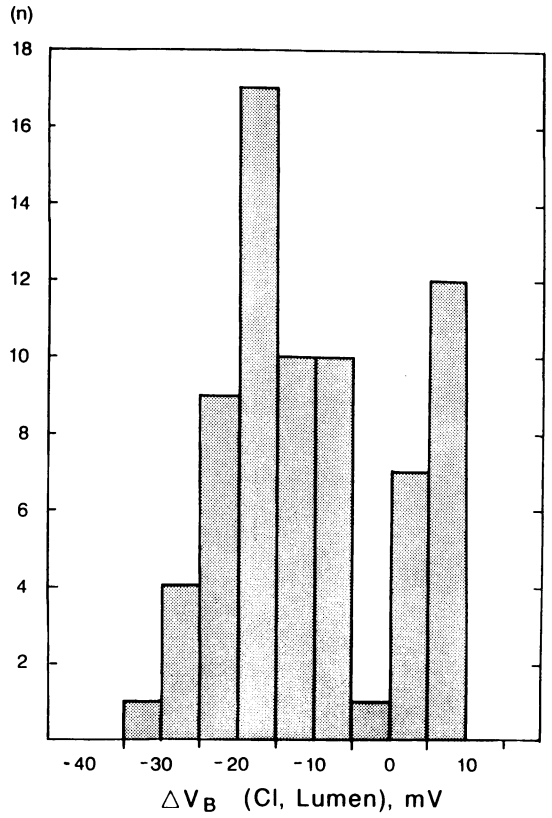

Figure 3. Frequency distribution of voltage deflection (ΔV_B) upon reduction of perfusate Cl^- concentration in the IC cells of the CCD. Positive values of ΔV_B indicate depolarization of the basolateral membrane, whereas negative values indicate hyperpolarization.

The V_B was unaffected by this maneuver, indicating that there is no appreciable K^+ conductance in the apical membrane.

The conductive properties of the basolateral membrane of α-IC cells were also assessed by observing deflection of V_B upon abrupt changes in Cl^- or K^+ concentration in the bath. Typical tracings are shown in Fig. 4 and the data are summarized in Fig. 5 and Table III. Upon changing the bath Cl^- from 120 to 12 mM, V_B rapidly deflected by 25.7±2.4 mV (n = 23) followed by a partial repolarization. Upon raising the Cl^- concentration back to 120 mM, V_B returned to the control value. On the other hand, the effect of the bath K^+ substitution on V_B was smaller. A 10-fold increase in the bath K^+ from 5 to 50 mM resulted in a small but significant depolarization of the basolateral membrane by 3.1±0.8 mV (n = 16). These characteristics are strikingly similar to those of the $OMCD_i$ cells as studied by Koeppen (25).

β-IC cells. The β-IC cells had a mean V_B of −28.9±1.3 mV (n = 70), a value that was not significantly different from that of the α-IC cells. The fR_A of the β-IC cell was also near unity and averaged 0.95±0.003 (n = 60), indicating that the apical membrane of this cell also does not have any appreciable ionic conductive pathways. As illustrated in Fig. 4 and summarized in Table III and Fig. 5, raising the perfusate K^+ from 5 to 50 mM had no effect on V_B. This response of the β-IC cell was similar to that of the α-IC cell. In contrast, an increase in the bath K^+ from 5 to 50 mM resulted in a small, but a significant depolarization of the basolateral membrane by 4.7±0.5 mV (n = 31). When Cl^- concentration in the bath was decreased from 120 to 12 mM, there was an immediate depolarization of V_B followed by a partial repolarization. The magnitude of this peak depolarization was 37.9±0.9 mV (n = 62), a value that was higher than that of the α-IC cell (25.7±2.4 mV, n = 23).

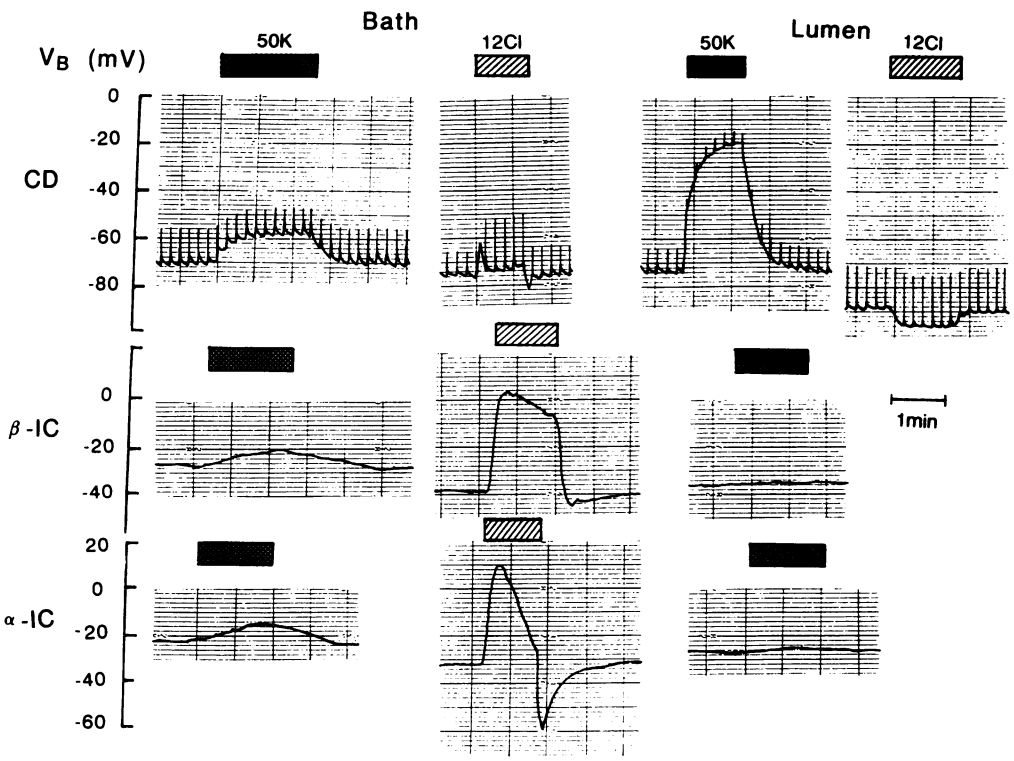

Figure 4. Typical tracings of V_B of three distinct cell types in the CCD upon lowering bath or perfusate Cl^- from 120 to 20 mM, and raising bath or perfusate K^+ from 5 to 50 mM. Voltage spikes are due to 50–100-nA constant current pulses at 10-s intervals.

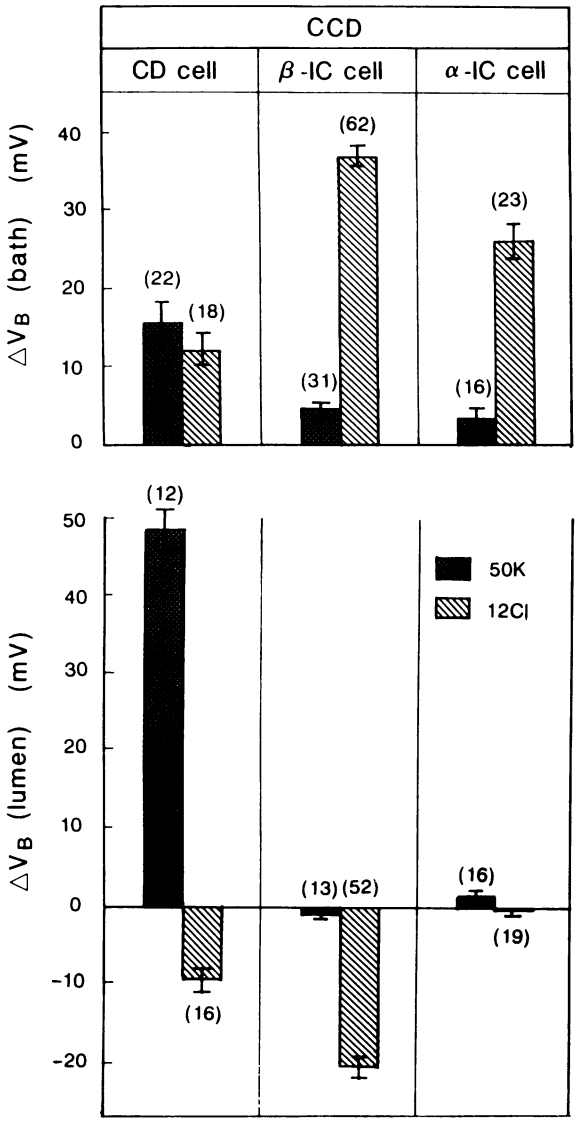

Figure 5. Deflections of V_B (ΔV_B) of three distinct cell types in the CCD, upon lowering bath or perfusate Cl^- and raising bath or perfusate K^+. All values are expressed as mean±SE. Positive values of ΔV_B indicate depolarization of the basolateral membrane; negative values indicate hyperpolarization.

The magnitude of the repolarization after a rapid depolarization in the β-IC cells seemed to be smaller than that observed in the α-IC cells.

Comparison of the electrical properties among CD cells, α- and β-IC cells in the CCD

To compare the electrical properties of the apical and basolateral membranes of the α- and β-IC cells with those of the CD cell, we also examined the behavior of the CD cell by ion substitution experiments. Representative tracings are also illustrated in Fig. 4 and the data are summarized in Table III and Fig. 5.

A 10-fold decrease in the luminal Cl^- resulted in a significant hyperpolarization of the basolateral membrane by 9.6±1.4 mV (n = 16). A 10-fold increase in the luminal K^+ caused a rapid depolarization of the basolateral membrane by 48.3±2.7 mV (n = 12), suggesting that the apical membrane of the CD cell was conductive for K^+. Upon lowering the bath Cl^- from 120 to 12 mM, the basolateral membrane was rapidly depolarized by 12.0±1.7 mV (n = 18) and then repolarized to a new steady state level. A mirror image response was observed when Cl^- concentration in the bath was returned to its control level. When the bath K^+ concentration was increased, the basolateral membrane of the CD cell was also depolarized by 16.3±2.7 mV (n = 22).

Thus, ion substitutions of Cl^- or K^+ in the lumen or bath led us to characterize electrical properties among the three distinct cell types of the CCD. To further define the features of these three distinct cell types of the CCD, V_B and its peak response (ΔV_B) upon reducing lumen or bath Cl^-, observed in the same cells, are plotted on three-dimensional scales (Fig. 6). It is clear from this figure that three distinct cell types can be separated without any overlap by using these parameters.

Identification and characterization of two subtypes of IC cells in the CNT

Yoshitomi et al. (4) identified the IC cell in the CNT segment according to the criteria described previously (8, 18, 25), and described membrane properties of the CNT. In the present study, we confirmed their observation and extended our study to identify the subtypes of the IC cell in the CNT. The mean values of V_B and fR_A of IC cells were −25.1±1.3 mV (n = 36) and 0.92±0.01 (n = 11), respectively, which are contrast to those of CNT cells (V_B −77.4±1.1 mV, n = 51; fR_A 0.48±0.03,

Table III. Effects of Bath and Perfusate Ion Substitutions on V_B of CD Cells, β-IC, and α-IC Cells in the CCD

		CD cell				β-IC cell				α-IC cell			
Ion	Concn.	n	Control	Experimental	Δ	n	Control	Experimental	Δ	n	Control	Experimental	Δ
	mM						*mV*						
Bath													
K^+	5 → 50	22	−79.6±2.0	−63.3±3.4	16.3±2.7*	31	−27.5±1.9	−22.8±1.9	4.7±0.5*	16	−27.6±2.9	−24.5±2.8	3.1±0.8*
Cl^-	120 → 12	18	−80.8±2.4	−68.8±2.9	12.0±1.7*	62	−27.3±1.3	−10.5±1.5	37.9±0.9*	23	−23.6±1.6	2.1±3.2	25.7±2.4*
Lumen													
K^+	5 → 50	12	−78.7±3.0	−30.4±2.6	48.3±2.7*	13	−26.9±3.9	−27.6±3.9	−0.76±0.4	16	−26.5±5.9	−25.0±5.6	1.5±0.7
Cl^-	120 → 12	16	−82.3±2.1	−91.9±1.9	9.6±1.4*	52	−29.7±1.8	−50.3±2.4	21.5±0.9*	19	−26.8±2.6	−26.4±2.6	0.4±0.5

Values are mean±SE. n, number of experiments; Δ, differences from the control values. * $P < 0.001$ compared to control values.

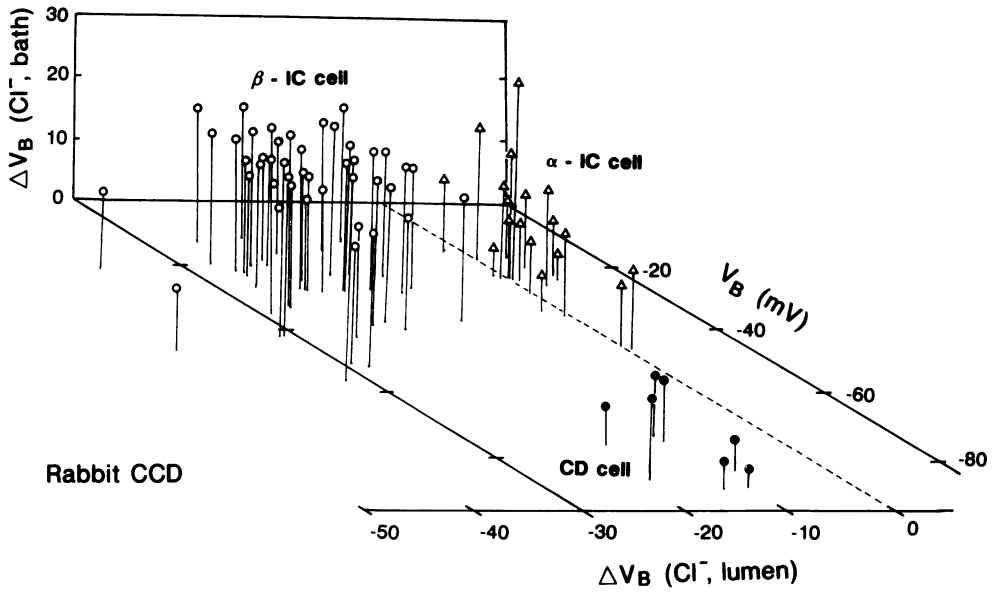

Figure 6. Three-dimensional plots of V_B and its peak response of V_B (ΔV_B) to lowering perfusate and bath Cl^- from 120 to 12 mM, in the same cells of the CCD. Positive values of ΔV_B indicate depolarization of the basolateral membrane, whereas negative values indicate hyperpolarization. (●) CD cells; (△) α-IC cells; (○) β-IC cells.

n = 9). Two different responses of V_B upon reduction of the perfusate Cl^- concentration were also noted in the CNT as well as in the CCD. However, the relative population of the β-IC cell is quite different. As illustrated in Fig. 7, and summarized in Fig. 8, 36 of 37 IC cells (97.3%) hyperpolarized the basolateral membrane by 19.6±2.7 mV, indicating that most IC cells in the CNT segment were identified as β-IC cells. Further studies were performed to characterize the electrical properties of the apical and basolateral membranes of the β-IC cell. Typical tracings are illustrated in Fig. 7 and the data are summarized in Fig. 8 and Table IV.

When the perfusate K^+ was increased from 5 to 50 mM, V_B of the β-IC was not affected. However, raising the bath K^+ resulted in a small depolarization of the basolateral membrane by 4.6±0.6 mV (n = 26). Upon reduction of the bath Cl^- from 120 to 12 mM, V_B was rapidly deflected by 31.3±2.8 mV (n = 19) followed by a slow repolarization. These responses of V_B of β-IC cells in the CNT were very similar to those of β-IC cells in the CCD.

Comparison of the electrical properties between the β-IC and CNT cells in the CNT. To compare the electrical properties of the β-IC cell with those of the CNT cell, we also exam-

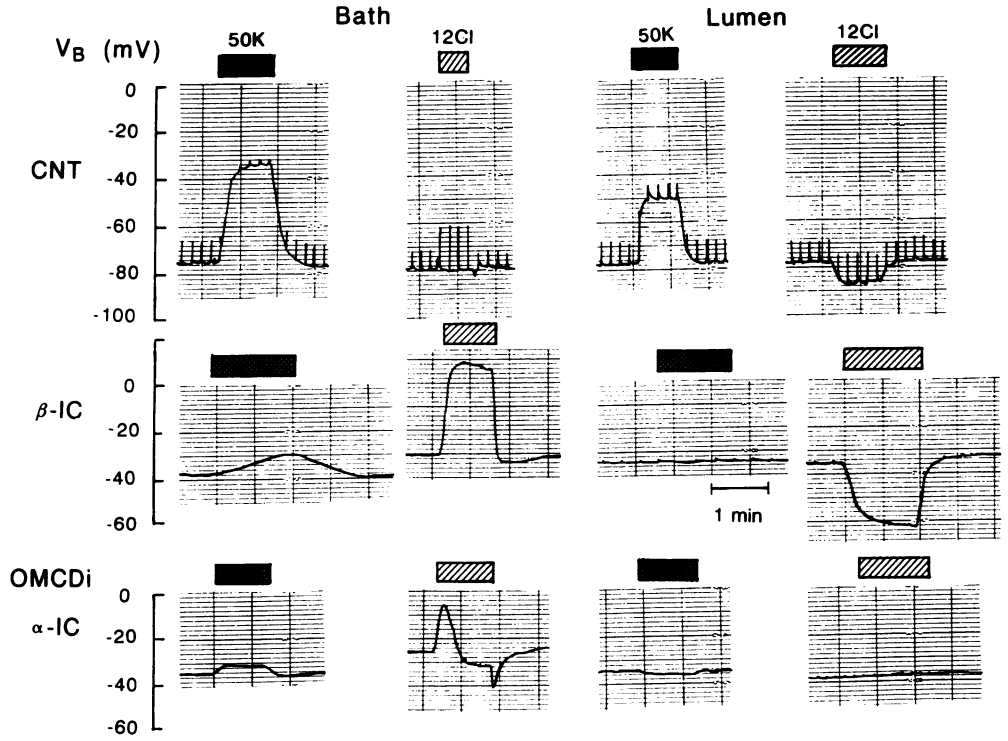

Figure 7. Typical tracings of V_B of CNT cells and β-IC cells in the CNT and α-IC cells in the $OMCD_i$, upon lowering bath or perfusate Cl^- from 120 to 12 mM, and raising bath or perfusate K^+ from 5 to 50 mM. Voltage spikes are due to 50–100-nA constant current pulses at 10-s intervals.

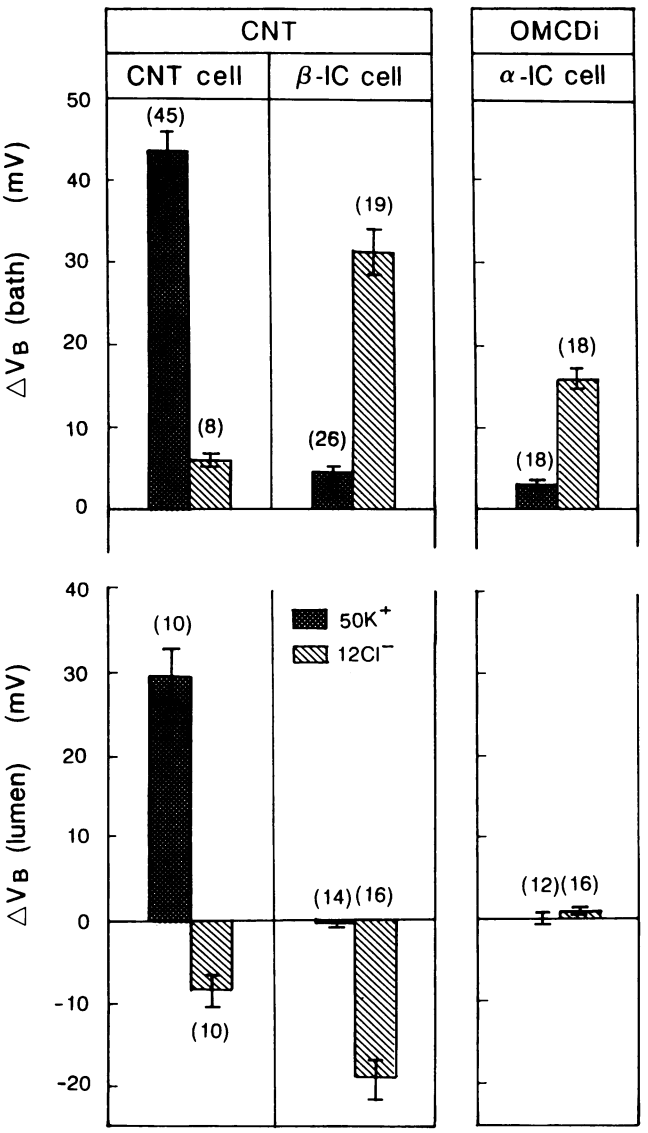

Figure 8. Deflections of V_B (ΔV_B) of CNT cells and β-IC cells in the CNT and α-IC cells in the $OMCD_i$, upon lowering bath or perfusate Cl^- and raising bath or perfusate K^+. All values are expressed as mean±SE. Positive values of ΔV_B indicate depolarization of the basolateral membrane, whereas negative values indicate hyperpolarization.

ined conductive properties of the CNT cell upon rapid ion substitutions of K^+ and Cl^- in the bath and perfusate. Typical tracings are also illustrated in Fig. 7 and summaries are also shown in Fig. 8 and Table IV. Raising perfusate K^+ had a significant deflection of V_B by 30.0±2.9 mV (n = 10), whereas lowering perfusate Cl^- hyperpolarized the basolateral membrane by 8.6±1.7 mV (n = 10). On the other hand, when the bath K^+ concentration was increased, V_B was rapidly deflected by 43.8±1.9 mV (n = 45). Also, when the bath Cl^- concentration was decreased, the basolateral membrane was rapidly depolarized by 5.8±1.3 mV (n = 8) within several seconds and then repolarized to a new steady-state value. This pattern was reversed upon returning to control conditions. These observations are compatible with those of Yoshitomi et al. (4). Thus, as shown in Fig. 7, we were able to discriminate sharply the β-IC cell from the CNT cell on the basis of its electrical properties of the apical as well as basolateral membranes.

Identification and characterization of the $OMCD_i$ cell in the $OMCD_i$

The cells of $OMCD_i$ had a mean of V_B of −29.1±2.3 mv (n = 19). The fR_A was near unity (0.96±0.01, n = 19). These values are similar to those reported by Koeppen (25), in this segment.

To determine the subtypes of the $OMCD_i$ cell, we observed the response of V_B upon reduction of the perfusate Cl^- from 120 to 12 mM. As illustrated in Fig. 7 and summarized in Fig. 8, all $OMCD_i$ cells of 19 cells punctured in 12 $OMCD_i$ segments had no change in V_B. These results are in good agreement with those of Koeppen (25) in this segment. Therefore, the $OMCD_i$ segment appears to be composed of only an α-type H^+ secreting cell. Further characterization of the apical and basolateral membranes was performed by ion substitutions with K^+ or Cl^-. Typical tracings are also illustrated in Fig. 7 and the data are summarized in Fig. 8 and Table IV.

A 10-fold increase in the perfusate K^+ had no effect on V_B. However, a 10-fold increase in bath K^+ had a small, but a significant depolarization of the basolateral membrane by 2.7±0.4 mV (n = 18). A 10-fold decrease in the bath Cl^- also had a rapid depolarization of V_B of 15.8±1.4 mV (n = 18) followed by a partial repolarization. These results are also compatible with those of Koeppen (25). Thus, the electrical characteristics of the apical and basolateral membranes of the $OMCD_i$ cell were quite similar to those of the α-IC cell in the CCD.

Table IV. Effects of Bath and Perfusate Ion Substitutions on V_B of CNT Cells and β-IC Cells in the CNT and α-IC Cells in the $OMCD_i$

		CNT cell (CNT)				β-IC cell (CNT)				α-IC cell ($OMCD_i$)			
Ion	Concn	n	Control	Experimental	Δ	n	Control	Experimental	Δ	n	Control	Experimental	Δ
	mM						*mV*						
Bath													
K^+	5 → 50	45	−78.0±1.3	−34.2±2.2	43.8±1.9*	26	−26.7±1.8	−22.0±1.5	4.6±0.6*	18	−30.6±2.2	−27.8±2.3	2.7±0.4*
Cl^-	120 → 12	8	−76.6±2.8	−70.9±3.6	5.8±1.3‡	19	−22.6±2.0	8.6±4.2	31.3±2.8*	18	−29.5±2.4	−13.6±3.2	15.8±1.4*
Lumen													
K^+	5 → 50	10	−77.3±1.7	−47.3±3.2	30.0±2.9*	14	−28.5±2.9	−28.5±3.0	−0.07±0.4	12	−29.6±3.5	−29.6±3.3	0±0.8
Cl^-	120 → 12	10	−80.6±3.4	−89.2±3.4	−8.6±1.7*	16	−26.1±2.1	−45.7±3.2	−19.6±2.7*	16	−31.8±2.7	−31.0±2.5	0.4±0.7

Values are mean±SE. n, number of experiments; Δ, differences from the control values. * $P < 0.001$; ‡ $P < 0.01$ compared to control values.

Discussion

The results of this study indicate that we can identify α- and β-IC cells along the rabbit distal nephron segments by the intracellular microelectrode technique. This study was the first to demonstrate the electrophysiological properties of the β-IC cell and its distribution along the distal nephron segments.

Identification of IC cells. Morphologically defined IC cells are intermingled along the CNT and collecting duct system of the mammalian kidney (1). Microelectrode studies have defined the electrical properties of the apical and basolateral membranes of IC cells in the CNT (4) as well as collecting ducts from rabbits (5, 8, 9, 12, 18). The IC cells, including those in the $OMCD_i$, are defined electrophysiologically by a relatively low V_B and high fR_A near unity (4, 8, 18, 25). They are also characterized by the absence of any detectable Na^+ or K^+ conductive properties in the apical membrane, and the presence of a Cl^- conductance in the basolateral membrane (4, 8, 18, 25). In the present study, we confirmed those findings and regarded them as criteria to define the IC cells.

Differentiation of two subtypes of IC cells in the CCD. Two subtypes of IC cells have been identified in the mammalian collecting ducts, with several methods including electronmicroscopic (10), immunohistochemical (28, 29, 33), and optical fluorometric (34–36, 40) techniques.

Schwartz and Al-Awqati (41) have demonstrated that two functionally distinct subpopulations of IC cells existed in the rabbit CCD. One form which corresponds to the α-IC cell was capable of endocytosis of a fluorescent marker from the luminal side. Another type of the IC cell which corresponds to the β-cell was capable of endocytosis from the peritubular side. Furthermore, Schuster et al. (28), using monoclonal antibody to human red blood cell anion exchanger, band 3 protein, and peanut lectin binding, have demonstrated two subtypes of IC cells in the rabbit CCD. They noticed that some IC cells bound peanut lectin but not antibody to band 3 protein, whereas others had band 3 protein, but not peanut lectin binding. Peanut lectin-positive band 3-negative cells were supposed to be β-IC cells, whereas peanut lectin-negative band 3-positive cells were supposed to be α-IC cells.

Recently, Weiner and Hamm (36), using pH-sensitive dye, acetoxy-methyl ester of 2′,7′-bis (carboxyethyl)-5(6)-carboxyfluorescein (BCECF-AM), differentiated the IC cell from the CD cell in the rabbit CCD, on the basis of the fact that luminally loaded BCECF-AM resulted in intense uptake into IC cells, whereas basolaterally loaded BCECF-AM resulted in apparent homogeneous uptake into all cells. Moreover, they identified two subtypes of IC cells by fluorescent labeling. β-IC cells were identified with fluorescein isothiocyanate-labeled peanut agglutinin, whereas α-IC cells were identified by endocytosis of luminal tetramethyl-rhodamine isothiocyanate-labeled dextran.

More recently, two subpopulations of IC cells in the rabbit CCD perfused in vitro were identified based on the cell alkalinization followed by a basolateral or luminal Cl^- removal (34, 35). β-IC cells were identified by removing Cl^- from the lumen, which causes cell alkalinization via the apical Cl^-/HCO_3^- anion exchanger. In contrast, α-IC cells were identified based on a cell alkalinization via the basolateral Cl^-/HCO_3^- exchanger in response to basolateral Cl^- removal.

In the present study, two subtypes of the IC cells were differentiated by the response of V_B upon reduction of the perfusate Cl^-. The observations are along the line of the proposed cell models. Some IC cells caused hyperpolarization of the basolateral membrane. This type of cells may be β-IC cells because they do have a Cl^- entry step across the apical membrane (see below). The rest of the IC cells are suggested to be α-IC cells, because they are assumed to have no Cl^- entry step at the apical membrane and have a remarkably similar response of V_B to that of the cells obtained from the rabbit $OMCD_i$, which are thought to be equivalent to H^+-secreting cells.

Characterization of the α- and β-IC cells in the CCD. Since the values of fR_A are close to unity in both α- and β-IC cells, the resistance of the apical membrane of both subtypes greatly exceeds that of the basolateral membrane. The lack of V_B response to luminal K^+ substitution further indicates that the apical membrane of both subtypes does not have an appreciable K^+ conductance. Two subtypes differ with respect to the mechanisms of Cl^- entry across the apical membrane. In α-IC cells, luminal Cl^- substitution has no effect on V_B. This finding is consistent with that reported by Koeppen (25) in the rabbit $OMCD_i$. Thus, it seems that the apical membrane of α-IC cells of the CCD does not contain a Cl^- conductance, as well. However, the existence of a small Cl^- conductance in the apical membrane cannot be ruled out, because it is difficult to detect the conductive properties of the high-resistance barrier in the apical membrane.

In contrast, basolateral membrane of β-IC cells hyperpolarized upon luminal Cl^- substitution, indicating the presence of some Cl^- entry steps at the apical membrane. The mechanisms of a Cl^- entry step across the apical membrane of the β-IC cells are not clear at the present time, but several possibilities should be considered. The first may involve a Cl^-/HCO_3^- exchanger at the apical membrane of the β-IC cells. Upon reduction of luminal Cl^-, the Cl^- entry into the cell via a Cl^-/HCO_3^- exchanger at the apical membrane should be decreased, resulting in a reduction in intracellular Cl^- activity, which in turn would hyperpolarize the basolateral membrane by increasing Nernst equilibrium potential for Cl^-. However, it is not known whether the Cl^-/HCO_3^- exchange involves an electroneutral or electrogenic mechanism. The second mechanism may be a conductive pathway for Cl^- at the apical membrane. Since the fR_A of the β-IC cell is so high, it is unlikely that the apical membrane has any appreciable ion conductances. In fact, we could not detect any initial depolarization spike upon reduction in luminal Cl^-. However, the presence of a small Cl^- conductance cannot be excluded. A third mechanism may involve a Cl^-/HCO_3^- exchanger in parallel with a Cl^- conductive pathway at the apical membrane of the β-IC cell. Finally, we cannot exclude a possible contribution of HCO_3^--independent Cl^- entry mechanisms including an active Cl^- transport in the apical membrane. Further detailed studies will be required to solve the mechanisms of a Cl^- entry at the apical membrane of the β-IC cell.

In contrast to the apical membrane, the basolateral membrane of both subtypes of IC cells contains similar electrical properties. In both subtypes, an initial rapid depolarization of the basolateral membrane followed by a slow repolarization was observed upon changing bath Cl^-. Also, a small depolarization of the basolateral membrane of both subtypes was found upon raising bath K^+. It is not known at present time

whether this response is either due to an appreciable K^+ conductance at the basolateral membrane or due to circular current loops across the epithelium generated by the change in V_T upon raising bath K^+ concentration on the CD cell.

Characterization of the CD cell in the CCD. In previous papers (5, 8, 12), the CD cell in the rabbit CCD was distinguished by a relatively high V_B and a low fR_A, and characterized by a large K^+ conductance and a small Na^+ conductance in the apical membrane, and Cl^- and K^+ conductances in the basolateral membrane. In the present study, we arrived at the same conclusions. It was also demonstrated that upon reduction of luminal Cl^-, the basolateral membrane of the CD cell was significantly hyperpolarized, suggesting the presence of a Cl^- entry pathway at the apical membrane. This finding is similar to that reported by Sansom et al. (42). They have proposed that a neutral Cl^-/HCO_3^- exchange mechanism also exists in the apical membrane of the CD cell. Further studies will be needed to define the Cl^- entry pathways at the apical membrane.

Identification and characterization of two subtypes of IC cells in the CNT. Morphologic (1, 6) and electrophysiologic (4) studies demonstrated that the CNT segment is composed of at least two cell types, the CNT and IC cells. Although Yoshitomi et al. (4) reported electrophysiologic properties of the CNT cell, the function of the IC cell in the CNT has not yet been established. In the present study, we found that almost all IC cells in the CNT displayed electrophysiologic characteristics similar to those of β-IC cells in the CCD. Thus, it is possible that the IC cell in the CNT may also exert HCO_3^- secretion. These findings are the first report to suggest the function of the IC cell in the CNT.

Characterization of the CNT cell in the CNT. Recent electrophysiologic studies (4) have shown that the CNT cell in the rabbit CNT has a large K^+ conductance and a small Na^+ conductance in the apical membrane, and a large K^+ conductance and a small Cl^- conductance in the basolateral membrane. The present studies confirmed those findings. In addition, we observed that lowering perfusate Cl^- caused the basolateral membrane to hyperpolarize. This observation suggests the presence of some Cl^- entry mechanisms at the apical membrane of the CNT cell as well. Further studies will be needed to solve the Cl^- entry mechanisms.

Identification and characterization of IC cells in the $OMCD_i$ segment. The $OMCD_i$ is assumed to be specialized in urine acidification and does neither participate in Na^+ or K^+ transport nor show any evidence for HCO_3^- secretion (14, 21, 43). In the present study, the $OMCD_i$ cell had a low V_B and a high fR_A close to unity, and was characterized by the absence of any detectable K^+ or Cl^- conductance in the apical membrane and the presence of a Cl^--selective conductance in the basolateral membrane. These observations are consistent with Koeppen's electrophysiological data (25) in this segment. Moreover, recent immunocytochemical studies (28, 29) demonstrated that a Cl^-/HCO_3^- exchanger is located at the basolateral membrane whereas a H^+-ATPase pump is at the apical membrane. Thus, the $OMCD_i$ is supposed to be composed of H^+-secreting cells.

In contrast, morphologic studies of Ridderstrale et al. (14) suggested that the rabbit $OMCD_i$ is also consisted of heterogenous cells. Recent immunocytochemical studies (28, 30) have also supported this view.

In the present study, however, we could not demonstrate any heterogeneity in the $OMCD_i$ at least by the electrophysiological mean. Furthermore, since all membrane properties of the $OMCD_i$ cell are in excellent agreement with those of the α-IC cell in the CCD, we conclude that the $OMCD_i$ cell mainly, if not exclusively, secretes H^+ and is thus electrophysiologically identical to the α-IC cell of the CCD. These observations are consistent with those of Koeppen (25), and support the view of Hayashi et al. (43) who reported that Cl^- transport across the $OMCD_i$ by anion exchange was immeasurably low or nonexistent and not induced by in vivo metabolic alkalosis.

Axial heterogeneity of α- and β-IC cells. Fig. 9 shows the distributions of α- and β-IC cells along the rabbit distal nephron segments. 36 of 37 IC cells (97.3%) in the CNT were β-IC cells, whereas all of 19 $OMCD_i$ cells were α-IC cells in the $OMCD_i$. In contrast, in the CCD, 79 of 99 IC cells (79.8%) were β-IC cells. We had an impression that the population of the α-IC cells in the CCD tended to increase toward the boundary of the outer medulla.

Schwartz et al. (44), have reported that 22% of IC cells in the rabbit CCD were immunocytochemically identified as α-IC cells. Their figure corresponds very well with our electrophysiological data. Schuster et al. (28), using a monoclonal antibody to human red blood cell band 3 protein, have demonstrated that 29% of IC cells in the rabbit CCD were identical to be α-IC cells.

Furthermore, these two groups have also reported axial heterogeneity of α- and β-IC cells along the rabbit collecting ducts, that is, the number of β-IC cells was greater in the cortex, whereas the number of α-IC cells was greater in the outer medulla. Although they did not examine the CNT segment, our present results are consistent with their observations. If we consider all the segments tested, β-IC cells are

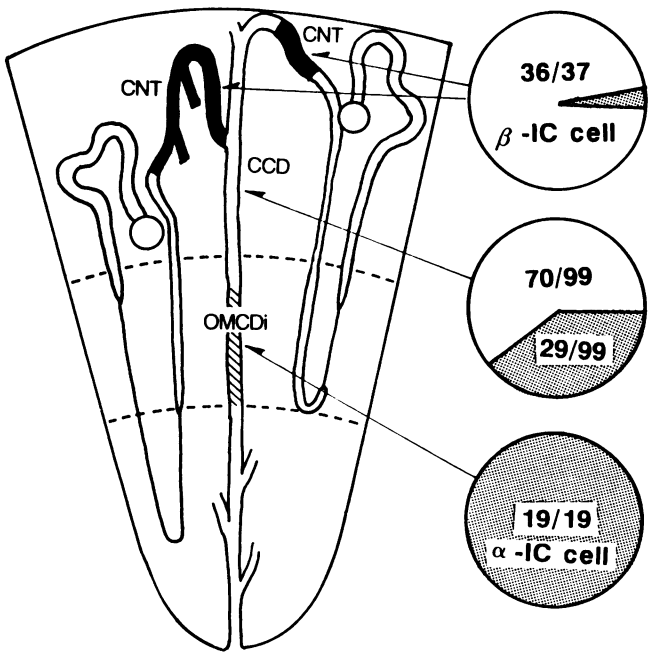

Figure 9. Distribution of two subtypes of IC cells along the distal nephron segments. The β-IC cells are the most predominant in the cortex, whereas the α-IC cells are predominant in the outer medullary portion.

predominant in earlier segments, whereas α-IC cells in the later segments.

Role of α- and β-IC cells in distal nephron segments. Several physiological significances would be proposed for the axial heterogeneity of two subtypes of IC cells along the distal nephron segments. The systemic acid-base status may influence the transport of H^+ and HCO_3^- in the distal nephron segments. The collecting duct system is responsible for reabsorption of a significant fraction of filtered HCO_3^- and for net H^+ secretion. In rats, depending on the experimental conditions, the fractional reabsorption of HCO_3^- between the distal tubule and the tip of the papilla may vary from 4% to 20% (45, 46). Of great importance is that the CCD can secrete H^+ or HCO_3^- depending on the acid–base status of the whole animal (47, 48), whereas the $OMCD_i$ always secretes H^+ (20–24). This views are consistent with our results. Thus, the α-IC cell in the $OMCD_i$ may play a critical role in the generation of pH gradient.

The HCO_3^- secretory system is of obvious importance in a herbivore like the rabbit, that usually secretes an alkaline urine. Another aspects which deserve emphasis are the studies of McKinney and Burg (47, 48). They reported that the isolated perfused CCD from normal and acid-loaded rabbits secretes H^+, whereas the CCD from HCO_3^--loaded rabbit secretes HCO_3^-. Star et al. (49) and Garcia-Austt et al. (50) also reported net HCO_3^- secretion in the CCD from deoxycorticosterone-treated rats and rabbits. Ishibashi et al. (24) observed that the steady-state luminal pH in stop-flow condition in the rabbit CCD was alkaline and was only slightly decreased after a bath pH reduction, supposing that HCO_3^- secretion may be the most important role of the CCD. From these observations, HCO_3^- secretion by β-IC cells in the CNT as well as CCD segments may be a physiologically important response to net alkali intake or to metabolic alkalosis. Alternatively, β-IC cells may be necessary for Cl^- absorption coupled with HCO_3^- secretion (49–51).

In summary, by using cable analyses and intracellular microelectrodes we have clearly defined two subpopulations of IC cells and characterized their electrical properties along the rabbit distal nephron segments.

Acknowledgments

We would like to express our thanks to Dr. G. Giebisch for his continuous stimulation in our pursuit of this work. We also thank Miss H. Hosaka for excellent technical assistance and Miss K. Ohtomo for expert secretarial work in preparing the manuscript.

This work was supported in part by grants from the Japanese Kidney Foundation (Jinkenkyukai), the Ministry of Education, Science and Culture of Japan (Grant-in-Aid for Encouragement of Young Scientists, No. 63770419; Grant-in-Aid for Scientific Research, No. 01570366), and Salt Science Foundation (No. 8910).

References

1. Kaissling, B., and W. Kriz. 1979. Structural analysis of the rabbit kidney. *Adv. Anat. Embryol. Cell Biol.* 56:1–123.

2. Imai, M. 1979. The connecting tubule: a functional subdivision of the rabbit distal nephron segments. *Kidney Int.* 15:346–356.

3. Shimizu, T., K. Yoshitomi, M., Nakamura, and M. Imai. 1988. Site and mechanism of action of trichlormethiazide in rabbit distal nephron segments perfused in vitro. *J. Clin. Invest.* 82:721–730.

4. Yoshitomi, K., T. Shimizu, and M. Imai. 1988. Functional cellular heterogeneity in the rabbit connecting tubule. *Kidney Int.* 33:430. (Abstr.)

5. Koeppen, B. M., B. A. Biagi, and G. H. Giebisch. 1983. Intracellular microelectrode characterization of the rabbit cortical collecting duct. *Am. J. Physiol.* 244:F35–F47.

6. Stanton, B., D. Biemesderfer, J. Wade, and G. Giebisch. 1981. Structural and functional study of rat distal nephron: effects of potassium adaptation and depletion. *Kidney Int.* 19:36–48.

7. Muto, S., S. Sansom, and G. Giebisch. 1987. Effects of high K diet on electrical properties of cortical collecting ducts from adrenalectomized rabbit. *J. Clin. Invest.* 81:376–380.

8. Muto, S., G. Giebisch, and S. Sansom. 1987. Effects of adrenalectomy on CCD: evidence for differential response of two cell types. *Am. J. Physiol.* 253:F742–F752.

9. Schlatter, E., and J. A. Schafer. 1987. Electrophysiological studies in principal cells of rat cortical collecting tubule: ADH increases the apical membrane Na^+ conductance. *Pflügers Arch. Eur. J. Physiol.* 409:81–92.

10. Madsen, K. M., and C. C. Tisher. 1986. Structural-functional relationships along the distal nephron. *Am. J. Physiol.* 250:F1–F15.

11. O'Neil, R., and R. A. Hayhurst. 1985. Functional differentiation of cell types of cortical collecting duct. *Am. J. Physiol.* 248:F449–F453.

12. O'Neil, R. G., and S. C. Sansom. 1984. Electrophysiological properties of cellular and paracellular conductive pathways of the rabbit cortical collecting duct. *J. Membr. Biol.* 82:281–295.

13. O'Neil, R. G., and S. I. Helman. 1977. Transport characteristics of renal collecting tubules: influences of DOCA and diet. *Am. J. Physiol.* 233:F544–F558.

14. Ridderstrale, Y., M. Kashgarian, B. Koeppen, G. Giebisch, D. Stetson, T. Ardito, and B. Stanton. 1988. Morphological heterogeneity of the rabbit collecting duct. *Kidney Int.* 34:655–670.

15. Stokes, J. B., M. J. Ingram, A. D. Williams, and D. Ingram. 1981. Heterogeneity of the rabbit collecting tubule: localization of mineralocorticoid hormone action to the cortical portion. *Kidney Int.* 20:340–347.

16. Helman, S. I., and R. G. O'Neil. 1877. Model of active transepithelial Na and K transport of renal collecting tubules. *Am. J. Physiol.* 233:F559–F571.

17. Stokes, J. B. 1982. Ion transport by the cortical and outer medullary collecting tubule. *Kidney Int.* 22:473–484.

18. Koeppen, B. M. 1986. Conductive properties of the rabbit outer medullary collecting duct: outer stripe. *Am. J. Physiol.* 250:F70–F76.

19. Schwartz, G. J., J. Barasch, and Q. Al-Awqati. 1985. Plasticity of functional epithelial polarity. *Nature (Lond.).* 3182:368–371.

20. Laski, M. E., and N. E. Kurtzman. 1983. Characterization of acidification in the cortical and medullary collecting tubule of the rabbit. *J. Clin. Invest.* 72:2050–2059.

21. Lombard, W. E., J. P. Kokko, and H. R. Jacobson. 1983. Bicarbonate transport in cortical and outer medullary collecting tubules. *Am. J. Physiol.* 244:F289–F296.

22. Stone, D. K., D. W. Seldin, J. P. Kokko, and H. R. Jacobson. 1983. Anion dependence of rabbit medullary collecting duct acidification. *J. Clin. Invest.* 71:1505–1508.

23. Stone, D. K., D. W. Seldin, J. P. Kokko, and H. R. Jacobson. 1983. Mineralocorticoid modulation of rabbit medullary collecting duct acidification. *J. Clin. Invest.* 72:77–83.

24. Ishibashi, K., S. Sasaki, N. Yoshiyama, T. Shiigai, and J. Takeuchi, 1987. Generation of pH gradient across the rabbit collecting duct segments perfused in vitro. *Kidney Int.* 31:930–936.

25. Koeppen, B. M. 1985. Conductive properties of the rabbit outer medullary collecting duct: inner stripe. *Am. J. Physiol.* 248:F500–F506.

26. Stetson, D. L., and P. R. Steinmetz. 1985. α and β types of carbonic anhydrase-rich cells in turtle bladder. *Am. J. Physiol.* 249:F553–F565.

27. Schwartz, G. J., and Q. Al-Awqati. 1986. Regulation of transep-

ithelial H^+ transport by exocytosis and endocytosis. *Annu. Rev. Physiol.* 48:153–161.

28. Schuster, V. L., S. M. Bonsib, and M. L. Jennings. 1986. Two types of collecting duct mitochondria-rich (intercalated) cells: lectin and band 3 cytochemistry. *Am. J. Physiol.* 251:C347–C355.

29. Brown, D., S. Hirsch, and S. Gluck. 1988. Localization of a proton-pumping ATPase in rat kidney. *J. Clin. Invest.* 82:2114–2126.

30. Verlander, J. W., K. M. Madsen, D. S. Low, D. P. Allen, and C. C. Tisher. 1988. Immunocytochemical localization of band 3 protein in the rat collecting duct. *Am. J. Physiol.* 255:F115–F125.

31. Burnatowska-Hledin, M. A., and W. S. Spielman. 1988. Immunodissection of mitochondria-rich cells from rabbit outer medullary collecting tubule. *Am. J. Physiol.* 254:F907–F911.

32. Holthofer, H., B. A. Schulte, G. Pasternack, G. J. Siegal, and S. S. Spicer. 1987. Three distinct cell populations in rat kidney collecting duct. *Am. J. Physiol.* 253:C323–C328.

33. Brown, D., S. Hirsch, and S. Gluck. 1988. An H^+-ATPase in opposite plasma membrane domains in kidney epithelial cell subpopulations. *Nature (Lond.).* 331:622–624.

34. Emmons, C. L., and J. B. Stokes. 1990. Mechanism of cAMP-induced HCO_3^- secretion by rabbit cortical collecting ducts (CCDs). *Kidney Int.* 37:536. (Abstr.)

35. Weiner, I. D., and L. L. Hamm. 1990. Regulation of intracellular pH in the rabbit cortical collecting tubule. *J. Clin. Invest.* 85:274–281.

36. Weiner, I. D., and L. L. Hamm. 1989. Use of fluorescent dye BCECF to measure intracellular pH in cortical collecting tubule. *Am. J. Physiol.* 256:F957–F964.

37. Burg, M., J. Grantham, M. Abramow, and J. Orloff. 1966. Preparation and study of fragments of single rabbit nephrons. *Am. J. Physiol.* 210:1293–1298.

38. Helman, S. I., J. J. Grantham, and M. B. Burg. 1971. Effect of vasopressin on electrical resistance of renal cortical collecting tubules. *Am. J. Physiol.* 220:1825–1832.

39. Wade, J. B., R. G. O'Neil, J. L. Pryor, and E. L. Boulpaep. 1979. Modulation of cell membrane area in renal collecting tubules by corticosteroid hormone. *J. Cell Biol.* 81:433–445.

40. Satlin, L. M., and G. J. Schwartz. 1989. Cellular remodeling of HCO_3^--secreting cells in rabbit renal collecting duct in response to an acidic environment. *J. Cell Biol.* 109:1279–1288.

41. Schwartz, G. J., and Q. Al-Awqati. 1985. Carbon dioxide causes exocytosis of vesicles containing H^+ pumps in isolated perfused proximal and collecting tubules. *J. Clin. Invest.* 75:1638–1644.

42. Sansom, S. C., E. J. Weinman, and R. G. O'Neil. 1984. Microelectrode assessment of chloride conductive properties of cortical collecting duct. *Am. J. Physiol.* 247:F291–F302.

43. Hayashi, M., V. L. Schuster, and J. B. Stokes. 1988. Absence of transepithelial anion exchange by rabbit $OMCD_i$ evidence against reversal of cell polarity. *Am. J. Physiol.* 255:F220–F228.

44. Schwartz, G. J., L. M. Satlin, and J. E. Bergmann. 1988. Fluorescent characterization of collecting duct cells: a second H^+-secreting type. *Am. J. Physiol.* 255:F1003–F1014.

45. Dubose, T. D., Jr., and M. S. Lucci. 1983. Effect of carbonic anhydrase inhibition on superficial and deep nephron bicarbonate reabsorption. *J. Clin. Invest.* 71:55–65.

46. Frommer, J. P., M. E. Laski, D. E. Wesson, and N. A. Kurzman. 1984. Internephronal heterogeneity for carbonic anhydrase independent bicarbonate reabsorption in the rat. *J. Clin. Invest.* 73:1034–1045.

47. McKinney, T. D., and M. B. Burg. 1978. Bicarbonate secretion by rabbit cortical collecting tubules in vitro. *J. Clin. Invest.* 61:1421–1427.

48. McKinney, T. D., and M. B. Burg. 1978. Bicarbonate absorption by rabbit cortical collecting tubules in vitro. *Am. J. Physiol.* 234:F141–F145.

49. Star, R. A., M. B. Burg, and M. A. Knepper. 1985. Bicarbonate secretion and chloride absorption by rabbit cortical collecting duct: role of chloride/bicarbonate exchange. *J. Clin. Invest.* 76:1123–1130.

50. Garcia-Austt, J., D. W. Good, M. B. Burg, and M. A. Knepper. 1985. Deoxycorticosterone-stimulated bicarbonate secretion in rabbit cortical collecting ducts: effects of luminal chloride removal and in vivo loading. *Am. J. Physiol.* 249:F205–F212.

51. Schuster, V. L., and J. B. Stokes. 1987. Cl^- transport by the cortical and outer medullary collecting duct. *Am. J. Physiol.* 253:F203–F212.